Dynamical creation of complex vector solitons in spinor Bose-Einstein condensates

Bo Xiong[1] and Jiangbin Gong[1,2,*]

[1]*Department of Physics and Centre for Computational Science and Engineering, National University of Singapore, 117542, Republic of Singapore*

[2]*NUS Graduate School for Integrative Sciences and Engineering, Singapore, 117597, Republic of Singapore*

(Received 18 October 2009; published 23 March 2010)

By numerical simulations of the Gross-Pitaevskii mean-field equations, we show that the dynamical creation of stable complex vector solitons in a homogeneous spin-1 Bose-Einstein condensate can be achieved by applying a localized magnetic field for a certain duration, with the initial uniform density prepared differently for the formation of different vector solitons. In particular, it is shown that stable dark-bright-dark vector solitons, dark-bright-bright vector solitons, and other analogous solutions can be dynamically created. It is also found that the peak intensity and the group velocity of the vector solitons thus generated can be tuned by adjusting the applied magnetic field. Extensions of our approach also allow for the creation of vector-soliton chains or the pumping of many vector solitons. The results can be useful for possible vector-soliton-based applications of dilute Bose-Einstein condensates.

DOI: 10.1103/PhysRevA.81.033618 PACS number(s): 03.75.Mn, 05.45.Yv

I. INTRODUCTION

In recent years, studies of spinor Bose-Einstein condensates (BECs) have attracted great interest. Via far-off-resonance optical trapping techniques, a spinor BEC can be realized in ^{23}Na [1,2] or ^{87}Rb [3,4] systems. Alternatively, a spinor BEC can be realized with an Ioffe-Pritchard magnetic trap by adiabatically reducing the magnetic bias field along the trap axis to zero [5]. In a spinor BEC, the spin comprises one extra degree of freedom, so that the order parameter of a BEC becomes a vector rather than a scalar quantity.

Because of the vector character of the order parameter and the important role of spin-relaxation collisions, spin-1 BECs can present two different ground-state phases; either a ferromagnetic phase or an antiferromagnetic (polar) phase [6,7]. This result has been extended to spin-2 BECs, which present an even richer variety of ground-state phases including, for example, the so-called cyclic phases [8,9]. Also due to the spin degree of freedom, spinor BECs have been shown to have a number of spin textures and topological excitations [10], including the formation of spin domains and spin-mixing dynamics [2], coreless vortices [6,7], and skyrmions or merons [11,12]. More related to this work, we note that great efforts have also been made to understand macroscopic nonlinear structures in spinor BECs, such as bright solitons [13–15], dark solitons [16,17], gap solitons [18], as well as more complex vector solitons that have both bright and dark components [19,20].

Given that the existence of at least one type of complex vector soliton (CVS) in spinor BECs is theoretically shown [19], it becomes interesting and useful to explore simple means for the creation of different types of CVSs in a spinor BEC. In this article, we consider the dynamical creation of stable CVSs by applying a localized magnetic field in a homogeneous spin-1 BEC in both ferromagnetic and antiferromagnetic cases. Evidently, at each spatial point, the applied field will induce internal Josephson tunneling between different components of the spinor BEC, and as a result the profile of the applied field must be shaped appropriately to ensure the emergence of CVSs. We obtain the appropriate profiles of the applied field by an intuitive approach, which is based on a small-amplitude expansion [19] of a static problem. As indicated by additional variational principle calculations, it can be expected that once a certain type of CVS is formed, it may continue to exist even after the applied field is turned off. We confirm our ideas by numerical simulations and linear stability analysis of the full Gross-Pitaevskii (GP) equations for a spin-1 BEC. In particular, we show the feasibility of creating different kinds of CVSs, including dark-bright-dark vector solitons (or analogously bright-dark-bright vector solitons) or dark-bright-bright vector solitons (or analogously bright-bright-dark vector solitons). We also find that we can easily tune the group velocity and the relative amplitudes of the different spin components of the CVS thus created by changing the parameters of the applied field. Moreover, we show that it is also possible to control the generated CVS number by creating a CVS chain, or by tuning the strength of the applied field periodically in time and hence pumping a controlled number of CVSs to the condensate after each cycle. These results should be useful for realizing a source of CVSs for future soliton-based applications of dilute BECs.

This article is organized as follows. In Sec. II, we present variational-principle considerations for CVSs in either antiferromagnetic or ferromagnetic spin-1 BECs. In Sec. III, we present and discuss a variety of results of the dynamical creation of stable CVSs. By analyzing the linearized GP equations, we also analytically discuss the modulational stability of each type of small-amplitude CVS. The particle-like nature of the CVS thus created is also demonstrated numerically. In Sec. IV, we summarize our findings. Some details in Appendix may be of interest to some readers, because they briefly explain how we reach a useful profile of a localized field for the dynamical creation of CVSs.

II. MODEL AND VARIATIONAL ANALYSIS

We consider a quasi-one-dimensional spinor $F = 1$ BEC confined by a cigar-shaped waveguide potential along the

*phygj@nus.edu.sg

 ©2010 The American Physical Society

x axial direction; that is, by a highly anisotropic trap with frequencies $\omega_x \ll \omega_\perp$. For such a spin-1 BEC, and at a temperature much lower than the critical temperature T_c, the mean-field description of the ultracold system with three spin components needs a vector order parameter $\Psi(\mathbf{x},t) = [\tilde{\psi}_1(\mathbf{x},t), \tilde{\psi}_0(\mathbf{x},t), \tilde{\psi}_{-1}(\mathbf{x},t)]^T$, with each component corresponding to the spin component $m_F = 1, 0, -1$. Because the transverse wave function $\psi_\perp(y,z)$ can be assumed to be the ground state of a harmonic potential, the mean-field wave functions can be taken as approximately separable [i.e., $\tilde{\psi}_{0,\pm1}(\mathbf{x},t) \approx \psi_{0,\pm1}(x,t)\psi_\perp(y,z)$]. One can then integrate out the transverse coordinates (y,z) first and obtain the following coupled one-dimensional GP equations [21],

$$\begin{aligned} i\hbar\partial_t\psi_1 &= -\frac{\hbar^2}{2m}\frac{\partial^2\psi_1}{\partial x^2} + B\psi_0 + B_z\psi_1 + c_0^{(1D)}(|\psi_1|^2 \\ &\quad + |\psi_0|^2 + |\psi_{-1}|^2)\psi_1 + c_2^{(1D)}(|\psi_1|^2 \\ &\quad + |\psi_0|^2 - |\psi_{-1}|^2)\psi_1 + c_2^{(1D)}\psi_{-1}^*\psi_0^2, \end{aligned} \tag{1a}$$

$$\begin{aligned} i\hbar\partial_t\psi_0 &= -\frac{\hbar^2}{2m}\frac{\partial^2\psi_0}{\partial x^2} + B^*\psi_1 + B\psi_{-1} + c_0^{(1D)}(|\psi_1|^2 \\ &\quad + |\psi_0|^2 + |\psi_{-1}|^2)\psi_0 + c_2^{(1D)}(|\psi_1|^2 \\ &\quad + |\psi_{-1}|^2)\psi_0 + 2c_2^{(1D)}\psi_{-1}\psi_0^*\psi_1, \end{aligned} \tag{1b}$$

$$\begin{aligned} i\hbar\partial_t\psi_{-1} &= -\frac{\hbar^2}{2m}\frac{\partial^2\psi_{-1}}{\partial x^2} + B^*\psi_0 - B_z\psi_{-1}^* + c_0^{(1D)}(|\psi_1|^2 \\ &\quad + |\psi_0|^2 + |\psi_{-1}|^2)\psi_{-1} + c_2^{(1D)}(|\psi_{-1}|^2 \\ &\quad + |\psi_0|^2 - |\psi_1|^2)\psi_{-1} + c_2^{(1D)}\psi_1^*\psi_0^2, \end{aligned} \tag{1c}$$

where m is the mass of the atom, $\mathbf{B} = (B_x, B_y, B_z)$, and $B \equiv (B_x - iB_y)/\sqrt{2}$ is due to Zeeman coupling with the magnetic field. In addition, in Eq. (1) the effective one-dimensional nonlinearity coefficients are given by $c_0^{(1D)} = c_0/(2\pi a_\perp^2)$ and $c_2^{(1D)} = c_2/(2\pi a_\perp^2)$, where $a_\perp = \sqrt{\hbar/(m\omega_\perp)}$ is the transverse harmonic oscillator length that defines the size of the transverse ground state and c_0 and c_2 account for spin-independent and spin-dependent collisions between identical spin-1 bosons, respectively. Specifically, c_0 and c_2 are given by

$$c_0 = \frac{4\pi\hbar^2(a_0 + 2a_2)}{3m}, \quad c_2 = \frac{4\pi\hbar^2(a_2 - a_0)}{3m}, \tag{2}$$

where a_0 and a_2 are the s-wave scattering lengths in the symmetric channels with total spin of two colliding atoms given by $F_{\text{tot}} = 0$ and $F_{\text{tot}} = 2$, respectively. Note that an $F = 1$ spinor BEC may be either ferromagnetic (such as the ^{87}Rb [22]), defined by $c_2 < 0$, or antiferromagnetic (polar, such as ^{23}Na [23]), defined by $c_2 > 0$.

It is convenient to rescale the time, length, and density by units of $\hbar(c_0^{(1D)}n_0)^{-1}$, $\hbar(mc_0^{(1D)}n_0)^{-1/2}$ and n_0 (where n_0 is the peak density of a BEC), respectively. After such a procedure, all variables below become dimensionless. We then obtain the following dimensionless GP equations,

$$\begin{aligned} i\partial_t\psi_1 &= \left[-\frac{1}{2}\frac{\partial^2}{\partial x^2} + \left(|\psi_1|^2 + |\psi_0|^2 + |\psi_{-1}|^2\right)\right]\psi_1 \\ &\quad + \delta(|\psi_1|^2 + |\psi_0|^2 - |\psi_{-1}|^2)\psi_1 \\ &\quad + \delta\psi_{-1}^*\psi_0^2 + B\psi_0 + B_z\psi_1, \end{aligned} \tag{3a}$$

$$\begin{aligned} i\partial_t\psi_0 &= \left[-\frac{1}{2}\frac{\partial^2}{\partial x^2} + \left(|\psi_1|^2 + |\psi_0|^2 + |\psi_{-1}|^2\right)\right]\psi_0 \\ &\quad + \delta(|\psi_1|^2 + |\psi_{-1}|^2)\psi_0 \\ &\quad + 2\delta\psi_{-1}\psi_0^*\psi_1 + B^*\psi_1 + B\psi_{-1}, \end{aligned} \tag{3b}$$

$$\begin{aligned} i\partial_t\psi_{-1} &= \left[-\frac{1}{2}\frac{\partial^2}{\partial x^2} + \left(|\psi_1|^2 + |\psi_0|^2 + |\psi_{-1}|^2\right)\right]\psi_{-1} \\ &\quad + \delta(|\psi_{-1}|^2 + |\psi_0|^2 - |\psi_1|^2)\psi_{-1} \\ &\quad + \delta\psi_1^*\psi_0^2 + B^*\psi_0 - B_z\psi_{-1}^*, \end{aligned} \tag{3c}$$

where we have defined

$$\delta \equiv \frac{c_2^{(1D)}}{c_0^{(1D)}} = \frac{a_2 - a_0}{a_0 + 2a_2}. \tag{4}$$

As such, $\delta < 0$ and $\delta > 0$ correspond to ferromagnetic and antiferromagnetic spinor BECs, respectively.

To gain insights into the possibility of forming different types of CVSs in the spin-1 BEC modeled above, we first employ simple variational calculations; a technique proved to be very useful in BEC soliton studies. The key step is to assume an ansatz for the mean-field wave functions $\psi_{0,\pm1}$ and then examine if there is a local energy minimum as the variational parameters vary.

Consider first the following ansatz:

$$\begin{pmatrix}\psi_1\\ \psi_0\\ \psi_{-1}\end{pmatrix} = \begin{bmatrix}\sqrt{(1-c)\,\mu - \frac{1}{2}a^2\exp\left(\frac{-x^2}{b^2}\right)}\\ a\exp\left(\frac{-x^2}{2b^2}\right)\\ \sqrt{c\mu + \left(\frac{1}{2} - 2c\right)a^2\exp\left(\frac{-x^2}{b^2}\right)}\end{bmatrix}, \tag{5}$$

where a and b are two dimensionless variational parameters that determine the amplitude and the width of the density profile, μ can be regarded as a fixed parameter to account for the homogeneous background associated with a dark-soliton component, and c is another important parameter that determines which type of CVS should be under consideration. To be physically relevant, we require $c \leqslant 1$ and $a \leqslant \sqrt{\mu}$. Clearly, if $c = 0.5$, Eq. (5) describes a dark-bright-dark density profile, with the $m_F = 1$ and $m_F = -1$ components displaying identical dark-soliton features, and the $m_F = 0$ component representing a bright density profile. On the other hand, if $c = 0$, then Eq. (5) evidently represents a dark-bright-bright density profile, with the $m_F = 0$ and $m_F = -1$ components displaying bright soliton features with unequal weights.

One may also propose similar ansätze to cover other types of CVSs, such as the bright-dark-bright and bright-bright-dark CVSs (as a matter of fact, a bright-bright-dark ansatz can be obtained by a mapping of $m_F \to -m_F$ from a dark-bright-bright ansatz). For example, we may consider the following alternative ansatz:

$$\begin{pmatrix}\psi_1\\ \psi_0\\ \psi_{-1}\end{pmatrix} = \begin{bmatrix}\frac{1}{\sqrt{2}}a\exp\left(\frac{-x^2}{2b^2}\right)\\ \sqrt{c\mu + (1-2c)\,a^2\exp\left(\frac{-x^2}{b^2}\right)}\\ \sqrt{(1-c)\,\mu + \left(c - \frac{1}{2}\right)a^2\exp\left(\frac{-x^2}{b^2}\right)}\end{bmatrix}. \tag{6}$$

In this case, when $c = 1$, Eq. (6) indeed describes a bright-dark-bright density profile; and when $c = 0$, Eq. (6) represents a bright-bright-dark density profile.

Let us now examine if the above ansätze of density profiles can be stable in the absence of a magnetic field. Only if the answer is yes can we then explore how to generate CVSs of a particular type of density profile in the spin-1 BEC. To that end, we calculate the total energy E of the spinor BEC system without the magnetic field:

$$E = \int dx \left[\left(\sum_{j=-1}^{1} \frac{1}{2} \frac{\partial \psi_j^*}{\partial x} \frac{\partial \psi_j}{\partial x} \right) + \frac{1}{2}(|\psi_1|^2 + |\psi_0|^2 + |\psi_{-1}|^2)^2 + \frac{\delta}{2}(|\psi_1|^2 + |\psi_0|^2 - |\psi_{-1}|^2)|\psi_1|^2 + \frac{\delta}{2}(|\psi_1|^2 + |\psi_{-1}|^2)|\psi_0|^2 + \frac{\delta}{2}(|\psi_{-1}|^2 + |\psi_0|^2 - |\psi_1|^2)|\psi_{-1}|^2 + \delta\left(\psi_1^* \psi_0^2 \psi_{-1}^* + \psi_1 (\psi_0^*)^2 \psi_{-1}\right) \right]. \quad (7)$$

Directly plugging the above ansatz (5) or (6) into Eq. (7), an expression for E may be obtained. However, this expression is rather complicated and hence will not be presented here. Nevertheless, by careful checking each term of E, we find that E can be divided into the following three terms:

$$E = E_k + E_c + E_s, \quad (8)$$

where E_k is the kinetic energy term, E_c (E_s) is a δ-independent (δ-dependent) term due to the atom interaction. Interestingly, for $\delta > 0$, such as in the ^{23}Na case, E is minimized by $c = 0.5$ (or 1) for the ansatz in Eq. (5) [or in Eq. (6)]. This suggests that it is possible to have dark-bright-dark or bright-dark-bright vector solitons for $\delta > 0$. By contrast, for $\delta < 0$, such as in the ^{87}Rb case, E is minimized by requiring $c = 0$ for either the ansatz in Eq. (5) or the ansatz in Eq. (6). This indicates that for $\delta < 0$, we should expect the existence of dark-bright-bright or bright-bright-dark vector solitons.

The renormalized energy landscapes of the CVS (after subtracting off the background fluid contribution) as a function of the variational parameters a and b can be easily mapped out numerically. If there is a local energy minimum, then it can be expected that a certain type of CVS will be stable. As an example, we present the energy profile associated with the ansatz in Eq. (5). Figures 1(a) and 1(b) display typical landscapes for the renormalized energy obtained from Eq. (7), for both dark-bright-dark ($c = 0.5$) and dark-bright-bright cases ($c = 0$). The divergence of the E curve at $b = 0$ in both Fig. 1(a) and Fig. 1(b) is due to the nonlinear interaction terms in Eq. (7). Clearly, there always exists a local energy minimum in both Figs. 1(a) and 1(b). Such an energy minimum is expected to trap a stable dark-bright-dark or a stable dark-bright-bright density profile. Also noteworthy is that the increasing rate of the renormalized energy with the width parameter b in the case of a dark-bright-dark solution is significantly slower than that for a dark-bright-bright solution. However, in either case, if the parameter a is small, then the dark-bright-dark or the dark-bright-bright solution shows rather slow increase in E as b increases. This suggests that the CVS with smaller a can suffer less excitation if b is not optimized. In other words, during the dynamical creation of such CVSs, a solution with a larger amplitude of the bright component should be prepared more carefully than that with a smaller amplitude. If not, large amount of matter-wave "radiation" can be emitted because of possible excitation of the BEC.

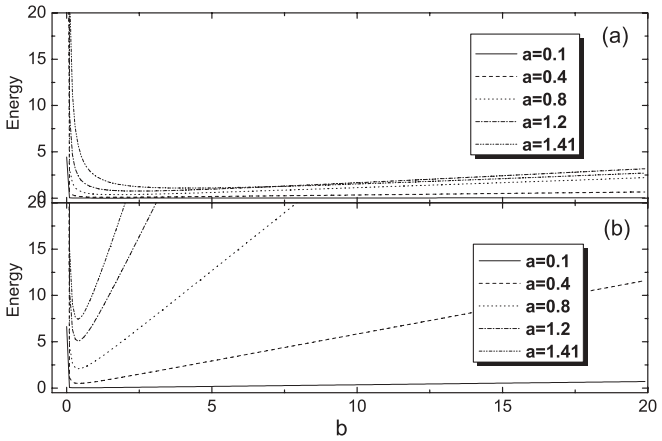

FIG. 1. Renormalized energy landscape as a function of the CVS-width parameter b, with the background intensity set at $\mu = 2$, for different values of the amplitude parameter a, obtained from Eq. (7). Panel (a) is for a dark-bright-dark solution with different values of a for an antiferromagnetic spin-1 BEC with $c = 0.5$ and $\delta = 3.14 \times 10^{-2}$ corresponding to ^{23}Na. Panel (b) is for a dark-bright-bright solution for a ferromagnetic case with $c = 0$ and $\delta = -4.66 \times 10^{-3}$ corresponding to ^{87}Rb. Here, and in all other figures, all variables are scaled and thus are dimensionless.

As seen below, the above results based on variational principle calculations provide an important guidance as to what initial mean-field wave function is needed for the creation of different kinds of CVSs. We also point out that the stability of different kinds of CVSs will be further elaborated below by a linear stability analysis.

III. DYNAMICAL CREATION AND LINEAR STABILITY ANALYSIS OF COMPLEX VECTOR SOLITONS

In this section, we shall show how to dynamically create different types of three-component CVSs by turning on a properly localized magnetic field for a certain duration. We shall also numerically reveal the particle-like nature of the CVS thus created after the magnetic field is turned off. In addition, when necessary, we will analytically discuss the linear stability of the dynamically created CVS. For simplicity, we choose a magnetic field along the x axis, such that in Eq. (3) $B_z = 0$ and $B = B_x$. To seek a useful profile of the magnetic field, our procedure is as follows: First, we ask what profile of an always-on weak field is beneficial in forming CVSs. This can be done by applying a small-amplitude asymptotic approximation, detailed in Ref. [19] for dark-bright-dark CVSs, to Eq. (3). Second, we intuitively assume that the field profile found this way can efficiently create a CVS if it is switched on for a certain duration.

For $\delta > 0$, our calculations, briefly outlined in Appendix, suggest that the following spatial dependence of a magnetic

field B (as one example) will help form CVSs. That is,

$$B_{\delta>0}=\beta\sqrt{\beta'}\left(\frac{\nu^{7/4}}{4\mu^{3/4}}\right)\mathrm{sech}(x\sqrt{\beta'\nu})\cos\left[x\left(\sqrt{\mu}-\frac{\sqrt{\nu}}{2}\right)\right], \tag{9}$$

where $\beta = 2\beta' - 1$ and $\nu = 16\delta\mu/5$. This special field profile reflects that, to form a CVS, the internal Josephson tunneling at each spatial point should be appropriately engineered. Interestingly, for $\delta < 0$, an analogous small-amplitude expansion procedure with a similar choice of free parameters suggests that the following profile of B can be used to support a CVS. Specifically,

$$B_{\delta<0} = \beta\sqrt{\beta'}\left[\frac{\nu^{7/4}}{(2\mu)^{3/4}}\right]\mathrm{sech}(x\sqrt{\beta'\nu})\cos\left[x\left(\sqrt{\mu}-\sqrt{\frac{\nu}{2}}\right)\right], \tag{10}$$

where $\beta = \beta' + 1$ and $\nu = 8|\delta|\mu/3$. Note that for both $\delta > 0$ and $\delta < 0$, the absolute amplitude of the field found is not essential because the turn-on time of the field is also a free parameter. Under a realistic experimental situation, the transverse harmonic oscillator frequency $\omega_\perp = 2\pi \times 230$ Hz, and the peak density $n_0 = 1 \times 10^8$ m^{-1}. Hence, for a ^{87}Rb (^{23}Na) condensate with $F = 1$ [22,23], our space and time units defined before correspond to 2.5 (1.8) μm and 2.4 (1.2) ms. The parameter δ defined in (4) takes values $\delta = -4.66 \times 10^{-3}$ and $\delta = +3.14 \times 10^{-2}$, for $F = 1$ ^{87}Rb and $F = 1$ ^{23}Na atoms, respectively. Below, we further choose $\mu = 2$, which accounts for the homogeneous background for the dark soliton component, which is the same choice as in Ref. [19].

The next issue is how to choose the appropriate initial mean-field wave function before we apply a localized magnetic field. To that end our early variational analysis becomes useful. In particular, for $\delta > 0$, if our goal is to create a stable dark-bright-dark CVS, then we may choose the following spatially uniform wave function:

$$\begin{pmatrix}\psi_1(0)\\ \psi_0(0)\\ \psi_{-1}(0)\end{pmatrix} = \begin{bmatrix}\sqrt{\frac{\mu}{2}}\\ 0\\ \sqrt{\frac{\mu}{2}}\end{bmatrix}. \tag{11}$$

This is because the ansatz in Eq. (5) reduces to the above state for $a = 0$ and $c = 0.5$. On the other hand, for $\delta < 0$, if our goal is to form a stable dark-bright-bright soliton, then the following initial state should be used:

$$\begin{pmatrix}\psi_1(0)\\ \psi_0(0)\\ \psi_{-1}(0)\end{pmatrix} = \begin{bmatrix}\sqrt{\mu}\\ 0\\ 0\end{bmatrix}, \tag{12}$$

which can be obtained by setting $a = 0$ and $c = 0$ in Eq. (5). In the following we will focus on the above two initially uniform states as our initial conditions. Similar considerations apply to the creation of bright-dark-bright and bright-bright-dark vector solitons.

After choosing the initial conditions just described, we then simulate Eq. (3) under a periodic boundary condition, with a large grid size of $L = 100$. The discrete steps in time and space used in our calculations are $\Delta t = 0.001$ and $\Delta x = 0.098$. A localized magnetic field as described in Eqs. (9) or (10) is suddenly turned on at time $t = 0$ and later switched off at time $t = t_f$. Our results confirm that the applied field can induce the formation of different types of stable CVSs. Below, we discuss our results in terms of the mass of each spin component as well as the spatial profile of different spin components. Here, the mass of one spin component is defined as the renormalized atom number after subtracting the background fluid contribution. That is, for a bright component, the mass of that component is just the scaled total atom number in that component. But for the mass of a dark component, it is defined as

$$N_{m_F} = \int (n_{m_F} - |\psi_{m_F}|^2)\, dx, \tag{13}$$

where m_F refers to the spin of a dark component and n_{m_F} is the background density.

A. Creation of dark-bright-dark vector solitons

Figure 2(a) shows the time dependence of the mass of each spin component, with the initial state given by Eq. (11) and the applied localized field given by Eq. (9). The time evolution of the density profile shown in Figs. 2(b) and 2(c) clearly indicates that a dark-bright-dark CVS pair moving in opposite directions is created. The propagation of the CVS thus created is seen to be highly stable—the distortion of the spatial profile can be hardly seen over a long time scale, and they can also undergo quasielastic collisions at $t = 170$, 340, etc. It is interesting to note that here a CVS pair, not just one single CVS, emerges from the dynamics. This is beyond a naive expectation from our small-amplitude expansion for a static problem (see Appendix). Although we are unable to fully explain such CVS-pair generation, we believe it is largely because our intuitive approach does not capture the inherent topological stability condition of the dark component of a CVS or the periodic boundary condition we used in our numerical simulations. Note that the mass of each spin component

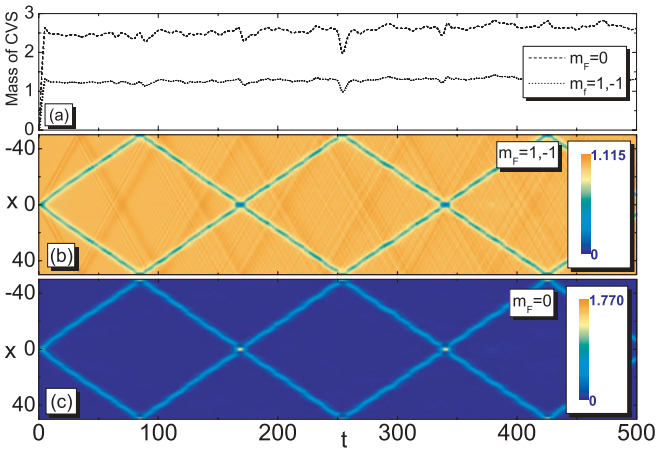

FIG. 2. (Color online) Dynamical creation of a dark-bright-dark vector soliton pair by applying a localized magnetic field satisfying Eq. (9) with $\delta = 3.14 \times 10^{-2}$ (corresponding to ^{23}Na), $\beta' = 10$, and $t_f = 5$. Panel (a) shows the time dependence of the soliton mass for each spin component. Panels (b) and (c) depict the time evolution of the particle density for $m_F = \pm 1$ and $m_F = 0$.

displays small oscillations, suggesting that the applied field does not have to completely balance the internal Josephson tunneling between different spin components. Note also that the properties for the $m_F = 1$ and $m_F = -1$ components remain completely the same during the time evolution. As such, the total magnetization of the BEC system remains absolutely zero.

We have also simulated analogous situations with different values of β' and t_f, which may be tuned in experiments. It is found that we can extensively manipulate the properties of the CVS thus created, such as the amplitude of the bright component as compared with the background density associated with the dark component, as well as the group velocity of the soliton. For example, for the CVS shown in Fig. 2(c), the ratio of the peak density of the bright component and the background fluid n_d (which is set to be 1) is ~0.94. But if we set $t_f = 2.0$ instead, then such a ratio reduces to about 0.4. The group velocity of the vector-soliton pair is also increased by 1.4 times if we set $t_f = 2.0$. The insignificant radiation of the matter wave in the course of CVS formation [see Fig. 2(b)] may be further suppressed by decreasing β' and t_f. It is also interesting to examine if the profile of the applied magnetic field can be made simpler; for example, using a profile proportional to the $\mathrm{sech}(x\sqrt{\beta' v})$ factor but without the $\cos[x(\sqrt{\mu} - \sqrt{v}/2)]$ factor in Eq. (9). It is found that the larger peak intensity of the created CVS, the more important this cosine factor would be.

To end this subsection, we note that the linear stability of the dark-bright-dark CVS for $\delta > 0$ has been demonstrated in detail in Ref. [19]. As such, it will not be repeated here. The same analysis for $\delta < 0$ predicts modulational instability for dark-bright-dark CVSs. However, as we shall see in the next subsection, for $\delta < 0$, dark-bright-bright CVSs can still have modulational stability.

B. Creation of dark-bright-bright vector solitons

For $\delta < 0$, our numerical simulations also confirm that other types of CVSs, such as dark-bright-bright vector solitons, can be successfully created by applying a localized magnetic field as prescribed in Eq. (10). The results are depicted in Fig. 3. From the time evolution of the spatial intensity profile of the BEC system, it is seen that a dark-bright-bright CVS pair with opposite velocity is formed from an initially uniform density described by Eq. (12). The CVS pair thus created can also propagate with little distortion, and can undergo a series of quasielastic collisions at $t = 155$, 310, 465, etc. As seen clearly from Fig. 3(a), here the oscillation in the soliton mass is much more significant than those seen in Fig. 2(a). Interestingly, it is seen that this does not much affect the stable propagation of the created CVS pair. This is a strong indication of the stability of the dynamically created CVS. Also interesting is that the mass of the bright component with $m_F = 0$ is always larger than that of the dark component with $m_F = -1$. This is because the latter is generated by the former through spin-exchange collisions. Analogous to the above-mentioned generation of dark-bright-dark CVSs, the properties of dark-bright-bright CVSs can also be extensively manipulated by tuning β' and t_f.

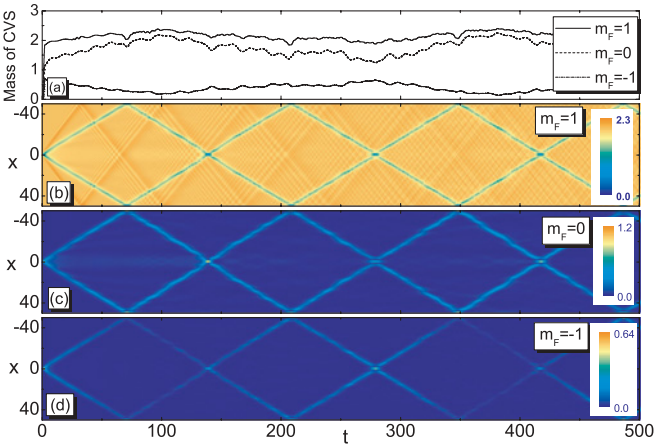

FIG. 3. (Color online) Dynamical creation of a dark-bright-bright vector soliton pair by applying a localized magnetic field satisfying Eq. (10) with $\delta = -4.66 \times 10^{-2}$ (which is ten times as much as the natural value of ^{87}Rb), $\beta' = 10$, and $t_f = 2$. Panel (a) shows the time dependence of the soliton mass for each spin component. Panels (b), (c), and (d) depict the time evolution of the particle density for $m_F = 1, 0, -1$.

To better understand the stability of dark-bright-bright CVSs created here, we now calculate the linear spectrum for a general small-amplitude excitation relative to a uniform background. Similar to the procedure in Ref. [19], we start our analysis by adopting the following ansatz:

$$\begin{aligned}\psi_{+1} &= \sqrt{n(x,t)}\exp[-i\mu(1+\delta)t + i\varphi(x,t)],\\ \psi_0 &= \phi_0(x,t)\exp[-i\mu(1+\delta)t],\\ \psi_{-1} &= \phi_{-1}(x,t)\exp[-i\mu(1-\delta)t],\end{aligned} \tag{14}$$

where $n(x,t)$ and $\varphi(x,t)$ are real functions that represent the density and phase of the fields ψ_{+1}, and ϕ_0 and ϕ_{-1} are complex functions. Such an ansatz solution is motivated by a uniform solution to Eq. (3) in the absence of a magnetic field. Substituting Eq. (14) into Eq. (3) for $B = B_z = 0$, one obtains

$$\begin{aligned}&\frac{i}{2}[\partial_t n + \partial_x(n\partial_x\varphi)] - n[\partial_t\varphi - (1+\delta)\mu + (1+\delta)n\\ &\quad + (1+\delta)|\phi_0|^2 + (1-\delta)|\phi_{-1}|^2] - n\left[\frac{1}{2}(\partial_x\varphi)^2\right.\\ &\quad \left. - \frac{1}{2\sqrt{n}}\partial_x^2\sqrt{n} + \frac{1}{\sqrt{n}}\delta\phi_0^2\phi_{-1}e^{-i\varphi-2i\delta\mu t}\right] = 0, \qquad (15a)\end{aligned}$$

$$\begin{aligned}&i\partial_t\phi_0 + \frac{1}{2}\partial_x^2\phi_0 - 2\delta\sqrt{n}\phi_0^*\phi_{-1}e^{i\varphi+2i\delta\mu t} - [(1+\delta)n\\ &\quad - (1+\delta)\mu + (1+\delta)|\phi_{-1}|^2 + |\phi_0|^2]\phi_0 = 0, \qquad (15b)\end{aligned}$$

$$\begin{aligned}&i\partial_t\phi_{-1} + \frac{1}{2}\partial_x^2\phi_{-1} - \delta\sqrt{n}\phi_0^2e^{-i\varphi-2i\delta\mu t} - [(1-\delta)n\\ &\quad - (1-\delta)\mu + (1+\delta)|\phi_{-1}|^2 + (1+\delta)|\phi_0|^2]\phi_{-1} = 0. \qquad (15c)\end{aligned}$$

As a common procedure of linear stability analysis, we now linearize the above equations around the continuous wave

solution of Eq. (12):

$$\begin{aligned} n &= \mu + \epsilon\tilde{n}, \\ \varphi &= \epsilon\tilde{\varphi}, \\ \phi_0 &= \epsilon\tilde{\phi}_0, \\ \phi_{-1} &= \epsilon\tilde{\phi}_{-1}, \end{aligned} \tag{16}$$

where ϵ is a small real parameter. Keeping only the $O(\epsilon)$ terms, Eqs. (15a)–(15c) lead to

$$i\left(\partial_t\tilde{n} + \mu\partial_x^2\tilde{\varphi}\right) - 2\mu\left[\partial_t\tilde{\varphi} + (1+\delta)\tilde{n} - \frac{1}{4\mu}\partial_x^2\tilde{n}\right] = 0, \tag{17a}$$

$$i\,\partial_t\tilde{\phi}_0 + \frac{1}{2}\partial_x^2\tilde{\phi}_0 = 0, \tag{17b}$$

$$i\,\partial_t\tilde{\phi}_{-1} + \frac{1}{2}\partial_x^2\tilde{\phi}_{-1} = 0. \tag{17c}$$

By further defining

$$\begin{aligned} \tilde{\phi}_0 &= \tilde{\phi}_{0,\mathrm{R}} + i\tilde{\phi}_{0,\mathrm{I}}, \\ \tilde{\phi}_{-1} &= \tilde{\phi}_{-1,\mathrm{R}} + i\tilde{\phi}_{-1,\mathrm{I}}, \end{aligned} \tag{18}$$

Eqs. (17a)–(17c) can be rewritten as the following:

$$\begin{aligned} &\partial_t\tilde{n} + \mu\partial_x^2\tilde{\varphi} = 0, \\ &\partial_t\tilde{\varphi} + (1+\delta)\tilde{n} - \frac{1}{4\mu}\partial_x^2\tilde{n} = 0, \\ &\partial_t\tilde{\phi}_{0,\mathrm{R}} + \frac{1}{2}\partial_x^2\tilde{\phi}_{0,\mathrm{I}} = 0, \\ &-\partial_t\tilde{\phi}_{0,\mathrm{I}} + \frac{1}{2}\partial_x^2\tilde{\phi}_{0,\mathrm{R}} = 0, \\ &\partial_t\tilde{\phi}_{-1,\mathrm{R}} + \frac{1}{2}\partial_x^2\tilde{\phi}_{-1,\mathrm{I}} = 0, \\ &-\partial_t\tilde{\phi}_{-1,\mathrm{I}} + \frac{1}{2}\partial_x^2\tilde{\phi}_{-1,\mathrm{R}} = 0. \end{aligned} \tag{19}$$

It is now evident that if we solve for $\tilde{\phi}_{0,\mathrm{R}}$ and $\tilde{\phi}_{-1,\mathrm{R}}$ from $\tilde{\phi}_{0,\mathrm{I}}$ and $\tilde{\phi}_{-1,\mathrm{I}}$, we finally arrive at the following three decoupled equations:

$$\partial_t^2\tilde{n} - (1+\delta)\mu\partial_x^2\tilde{n} + \tfrac{1}{4}\partial_x^4\tilde{n} = 0, \tag{20a}$$

$$\partial_t^2\tilde{\phi}_{0,\mathrm{R}} + \tfrac{1}{4}\partial_x^4\tilde{\phi}_{0,\mathrm{R}} = 0, \tag{20b}$$

$$\partial_t^2\tilde{\phi}_{-1,\mathrm{R}} + \tfrac{1}{4}\partial_x^4\tilde{\phi}_{-1,\mathrm{R}} = 0. \tag{20c}$$

These three decoupled equations directly give the following three dispersion relations

$$\omega_1^2 = (1+\delta)\mu k_1^2 + \frac{k_1^4}{4}, \tag{21a}$$

$$\omega_2^2 = \frac{k_2^4}{4}, \tag{21b}$$

$$\omega_3^2 = \frac{k_3^4}{4}, \tag{21c}$$

where $\omega_1, \omega_2, \omega_3$ are the excitation frequencies, and k_1, k_2, and k_3 are the associated perturbation wave vectors. Apparently, Eq. (21a) predicts a real frequency ω_1 and hence modulational stability for $\delta > -1.0$ (in our studied case, $\delta = -4.66 \times 10^{-3}$ for ^{87} Rb). Furthermore, Eqs. (21b) and (21c) indicate linear stability for any value of δ. Hence, so long as the amplitude of the created dark-bright-bright CVS is sufficiently small, the CVS as a vector excitation can remain linearly stable for $\delta > -1.0$.

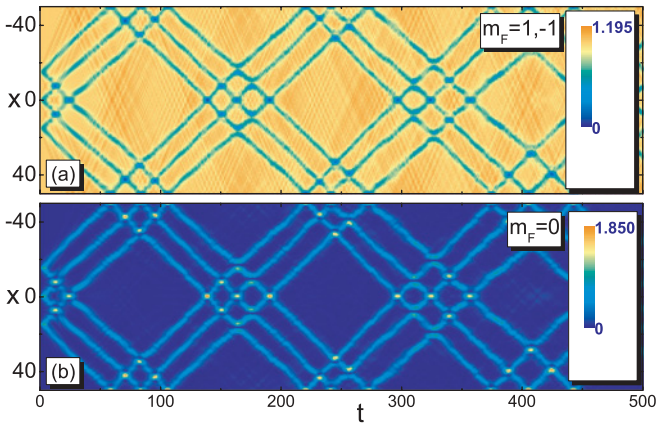

FIG. 4. (Color online) Dynamical creation of multiple dark-bright-dark vector solitons by applying a magnetic field profile repeating that of Eq. (9) three times, with the associated three peaks at $x = 0, \pm 15$. The other parameters are given by $\delta = 3.14 \times 10^{-2}$ (corresponding to ^{23}Na), $\beta' = 10$, and $t_f = 5$. Panels (a) and (b) depict the time evolution of the particle density for $m_F = \pm 1$ and for $m_F = 0$.

C. CVS chain and CVS pumping

A natural extension is to generate many CVSs at the same time, by applying a magnetic field localized at different regions. Our numerical simulations show that this is indeed possible. Figure 4 shows the generation of a dark-bright-dark CVS chain and their ensuing quasielastic collision dynamics. The profile of the applied magnetic field repeats

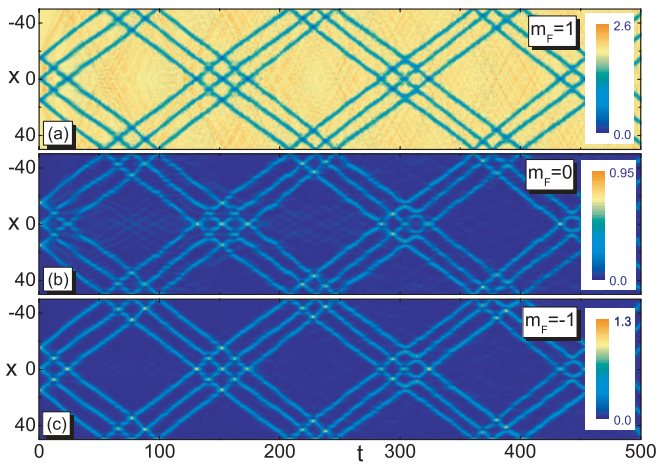

FIG. 5. (Color online) Dynamical creation of multiple dark-bright-bright vector solitons by applying a magnetic field profile repeating that of Eq. (10) three times, with the associated three peaks at $x = 0, \pm 15$. The other parameters are given by $\delta = -4.66 \times 10^{-3}$ (corresponding to ^{87}Rb), $\beta' = 250$, and $t_f = 2$. Panels (a), (b), and (c) depict the time evolution of the particle density for $m_F = 1$, $m_F = 0$, and $m_F = -1$.

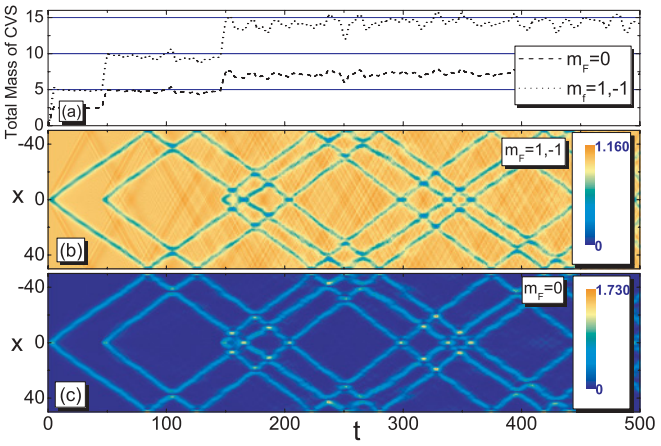

FIG. 6. (Color online) The pumping of dark-bright-dark vector soliton pairs into a spin-1 BEC, by periodically turning on and off an appropriate magnetic field profile. The pumping cycles start at $t = 0$, 45, 145 and the period of each control cycle is 5.0 in dimensionless time units. The other parameters are $\delta = 3.14 \times 10^{-2}$ (corresponding to ^{23}Na) and $\beta' = 10$. Panel (a) displays how the total mass of each spin component accumulates during the pumping process. The other panels depict the time evolution of the particle density for $m_F = \pm 1$ (b) and $m_F = 0$ (c).

that of Eq. (9) three times. Similarly, Fig. 5 depicts the formation of a dark-bright-bright CVS chain, with the applied magnetic field having three well-separated peaks described by Eq. (10).

What will happen if we periodically turn on and then turn off the magnetic field profile prescribed in Eqs. (9) and (10)? Our numerical simulation results for such situations are shown in Figs. 6 and 7, for the dark-bright-dark CVS and dark-bright-bright CVS cases, respectively. In either case, it is seen that the total mass of each CVS component, which is the sum of

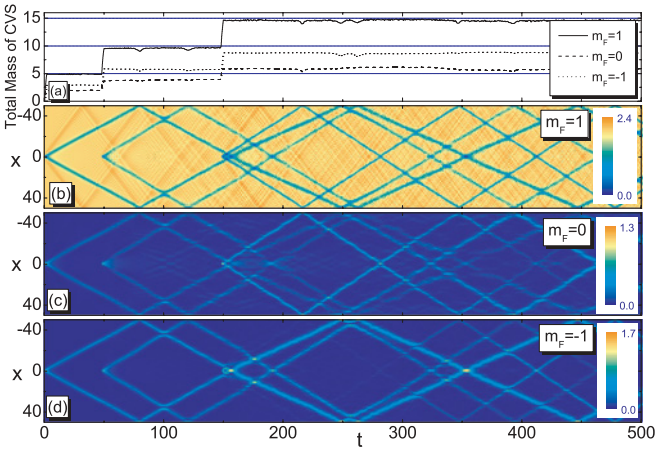

FIG. 7. (Color online) The pumping of dark-bright-bright vector soliton pairs into a spin-1 BEC, by periodically turning on and off an appropriate magnetic field profile. The pumping cycles start at $t = 0$, 48, 148 and the duration of each cycle is 2.0 in dimensionless time units. The other parameters are given by $\delta = -4.66 \times 10^{-3}$ (corresponding to ^{87}Rb) and $\beta' = 250$. Panel (a) displays how the total mass of each spin component accumulates during the pumping process. The other panels depict the time evolution of the particle density for $m_F = +1$ (b), $m_F = 0$ (c), and $m_F = -1$ (d).

the soliton mass for all CVS pairs created, is increased in a stepwise fashion. The sharp increase of the soliton mass occurs when the applied magnetic field is turned on in a new cycle. This clearly indicates a simple mechanism for a CVS pump. Though in Figs. 6 and 7 we only showed the pumping of two CVS pairs using two cycles, we checked that many more CVS pairs can be created in this fashion. We have also checked that we can even pump many CVS chains into the system by periodically modulating the magnetic field associated with the creation of a CVS chain.

IV. CONCLUSION

In this work, we have shown how to dynamically create complex and coherent vector excitations in spinor BECs by applying spatially localized fields. We showed that different types of CVSs, such as dark-bright-dark, dark-bright-bright vector solitons, and even their soliton chains, can be generated. Because many aspects of vector solitons in spinor BECs remain to be explored, having an experimentally feasible means for the generation of complex vector solitons will pave the way for vector-soliton based applications of BECs.

In demonstrating the generation of CVSs by applying a localized magnetic field, the field profile we proposed is based on considerations of a spinor BEC in the presence of a static magnetic field. Specifically, using a small-amplitude expansion similar to that in Ref. [19], we find the required field profile to support different types of CVSs, and then propose to use the field profile found to generate different types of CVSs. This intuitive approach is shown to work well—it even works for the generation of dark-bright-bright vector solitons, which are not previously examined in the context of spinor BECs. To confirm that such a new type of vector excitation is indeed stable, we have also explicitly performed a linear stability analysis for dark-bright-bright vector solitons.

ACKNOWLEDGMENTS

This work was supported by the start-up fund (WBS Grant No. R-144-050-193-101/133) and the NUS "YIA" fund (WBS Grant No. R-144-000-195-101), both from the National University of Singapore.

APPENDIX: ON THE PROFILE OF A LOCALIZED MAGNETIC FIELD FOR CVS GENERATION

In this appendix we briefly outline how we reach a reasonable spatial profile of B in Eq. (3), which is shown to lead to successful dynamical creation of different kinds of complex vector solitons. Without loss of generality, we consider here Eq. (3) for $\delta > 0$.

For the creation of a dark-bright-dark soliton, we start our analysis by adopting the following ansatz:

$$\psi_{\pm 1} = \sqrt{n(x,t)}\exp[-i\mu t + i\varphi(x,t)],$$
$$\psi_0 = \phi_0(x,t)\exp(-i\mu t), \tag{A1}$$

where ϕ_0 is a complex function, for a spin-1 BEC in a static magnetic field. Substituting (A1) into Eqs. (3), we obtain the

following equations:

$$\frac{i}{2}[\partial_t n + \partial_x(n\partial_x\varphi)] - n[\partial_t\varphi - \mu + 2n + (1+\delta)|\phi_0|^2] - n\left[\frac{1}{2}(\partial_x\varphi)^2 - \frac{1}{2\sqrt{n}}\partial_x^2\sqrt{n} + \delta\phi_0^2 e^{-2i\varphi}\right] - B\sqrt{n}\phi_0 e^{-i\varphi} = 0, \quad \text{(A2a)}$$

$$i\partial_t\phi_0 + \frac{1}{2}\partial_x^2\phi_0 - (2n - \mu + |\phi_0|^2)\phi_0 - 2\delta n(\phi_0 + \phi_0^* e^{2i\varphi}) - (B + B^*)\sqrt{n}e^{i\varphi} = 0, \quad \text{(A2b)}$$

$$\frac{i}{2}[\partial_t n + \partial_x(n\partial_x\phi)] - n[\partial_t\phi - \mu + 2n + (1+\delta)|\phi_0|^2] - n\left[\frac{1}{2}(\partial_x\phi)^2 - \frac{1}{2\sqrt{n}}\partial_x^2\sqrt{n} + \delta\phi_0^2 e^{-2i\varphi}\right] - B^*\sqrt{n}\phi_0 e^{-i\varphi} = 0, \quad \text{(A2c)}$$

where $B \equiv (B_x - iB_y)/\sqrt{2}$. Based on the consistency of Eqs. (A2a) with Eq. (A2c), one sees that the above ansatz requires B to be real. So we set $B_y = 0$.

To seek what profile of B can help form a stable dark-bright-dark vector soliton, we consider an approximate solution to the above Eq. (A2) by use of the following small-amplitude expansion:

$$n = (\mu/2) + \delta\rho(x,t), \quad \varphi = \delta^{1/2}\alpha(x,t),$$
$$\phi_0 = \delta^{3/4}q(x,t), \quad B = \delta^{\lambda}\tilde{B}(x,t), \quad \lambda \sim O(1), \quad \text{(A3)}$$
$$q \equiv q_1\cos(Kx - \Omega t) + iq_2\sin(Kx - \Omega t).$$

Noting that $|\delta|$ is rather small for both ^{23}Na and ^{87} Rb cases, we find $\lambda = 7/4$ and an equation for B:

$$i\partial_T q + \frac{1}{2}\partial_X^2 q - 2\rho q - \mu(q + q^*) - \tilde{B}\sqrt{2\mu} = 0, \quad \text{(A4)}$$

where $X = \sqrt{\delta}(x - \sqrt{\mu}t)$ and $T = \delta t$. We next take advantage of the following equations derived at other orders in δ in Ref. [19] for field-free cases:

$$\sqrt{\mu}\partial_X\alpha = 2\rho,$$
$$-\frac{i\sqrt{\mu}}{4}(2\partial_X\rho - \sqrt{\mu}\partial_X^2\alpha) - \sqrt{\frac{\mu}{2}}(\partial_T\alpha + |q|^2) = 0,$$
$$\Omega q_1 - \frac{K^2}{2}q_2 = 0, \quad -\frac{K^2}{2}q_1 + \Omega q_2 = 0,$$
$$-K\partial_X q_1 + \sqrt{\mu}\partial_X q_2 = 0, \quad -\sqrt{\mu}\partial_X q_1 + K\partial_X q_2 = 0,$$

with q and ρ set as sech functions with appropriate phases. We finally obtain from Eq. (A4) a (moving) spatial profile for B as follows:

$$B_{\delta>0} = \beta\sqrt{\beta'}\left(\frac{\nu^{7/4}}{4\mu^{3/4}}\right)\mathrm{sech}(x\sqrt{\beta'\nu})\cos\left[x\left(\sqrt{\mu} - \frac{\sqrt{\nu}}{2}\right)\right], \quad \text{(A5)}$$

where $\beta = 2\beta' - 1$ and $\nu = 16\delta\mu/5$. In obtaining Eq. (A5), we have also chosen the values of some free parameters of the order of unity. For realistic parameter values $\delta = +3.14 \times 10^{-2}$ (^{23}Na) and $\mu = 2$, we get $\nu = 0.20096$. If we further choose $\beta' = 10$ as in Fig. 2, we have $\beta'\nu = 2.0096$. For these parameters, the spatial profile of B is essentially a localized hyperbolic secant function, but with minor modifications arising from the cosine factor. As shown in our numerical simulations, such a profile is seen to be useful in the dynamical creation of dark-bright-dark solitons. Similar reasoning for $\delta < 0$ leads us to Eq. (10) as one sample solution.

[1] D. M. Stamper-Kurn, M. R. Andrews, A. P. Chikkatur, S. Inouye, H. J. Miesner, and W. Ketterle, Phys. Rev. Lett. **80**, 2027 (1998).

[2] J. Stenger *et al.*, Nature (London) **396**, 345 (1998).

[3] D. S. Hall, M. R. Matthews, J. R. Ensher, C. E. Wieman, and E. A. Cornell, Phys. Rev. Lett. **81**, 1539 (1998).

[4] M. S. Chang, C. D. Hamley, M. D. Barrett, J. A. Sauer, K. M. Fortier, W. Zhang, L. You, and M. S. Chapman, Phys. Rev. Lett. **92**, 140403 (2004).

[5] A. E. Leanhardt, Y. Shin, D. Kielpinski, D. E. Pritchard, and W. Ketterle, Phys. Rev. Lett. **90**, 140403 (2003).

[6] T. L. Ho, Phys. Rev. Lett. **81**, 742 (1998).

[7] T. Ohmi and K. Machida, J. Phys. Soc. Jpn. **67**, 1822 (1998).

[8] C. V. Ciobanu, S. K. Yip, and T. L. Ho, Phys. Rev. A **61**, 033607 (2000).

[9] M. Koashi and M. Ueda, Phys. Rev. Lett. **84**, 1066 (2000); M. Ueda and M. Koashi, Phys. Rev. A **65**, 063602 (2002).

[10] C. K. Law, H. Pu, and N. P. Bigelow, Phys. Rev. Lett. **81**, 5257 (1998).

[11] U. Al Khawaja and H. Stoof, Nature (London) **411**, 918 (2001).

[12] E. J. Mueller, Phys. Rev. A **69**, 033606 (2004).

[13] J. Ieda, T. Miyakawa, and M. Wadati, Phys. Rev. Lett. **93**, 194102 (2004); J. Phys. Soc. Jpn. **73**, 2996 (2004).

[14] L. Li, Z. Li, B. A. Malomed, D. Mihalache, and W. M. Liu, Phys. Rev. A **72**, 033611 (2005).

[15] W. Zhang, Ö. E. Müstecaplıoğlu, and L. You, Phys. Rev. A **75**, 043601 (2007).

[16] H. Pu, S. Raghavan, and N. P. Bigelow, Phys. Rev. A **63**, 063603 (2001).

[17] M. Uchiyama, J. Ieda, and M. Wadati, J. Phys. Soc. Jpn. **75**, 064002 (2006).

[18] B. J. Dabrowska-Wüster, E. A. Ostrovskaya, T. J. Alexander, and Y. S. Kivshar, Phys. Rev. A **75**, 023617 (2007).

[19] H. E. Nistazakis, D. J. Frantzeskakis, P. G. Kevrekidis, B. A. Malomed, and R. Carretero-Gonzalez, Phys. Rev. A **77**, 033612 (2008).

[20] X. X. Liu, H. Pu, B. Xiong, W. M. Liu, and J. B. Gong, Phys. Rev. A **79**, 013423 (2009).

[21] T. Isoshima, M. Nakahara, T. Ohmi, and K. Machida, Phys. Rev. A **61**, 063610 (2000).

[22] E. G. M. van Kempen, S. J. J. M. F. Kokkelmans, D. J. Heinzen, and B. J. Verhaar, Phys. Rev. Lett. **88**, 093201 (2002).

[23] N. N. Klausen, J. L. Bohn, and C. H. Greene, Phys. Rev. A **64**, 053602 (2001).